SF2A 2011
G. Alecian, K. Belkacem, R. Samadi and D. Valls-Gabaud (eds)

EARLY-TYPE GALAXIES: MASS-SIZE RELATION AT $Z \sim 1.3$ FOR DIFFERENT ENVIRONMENTS

A. Raichoor[1], S. Mei[1], S. A. Stanford[2], B. P. Holden[3], F. Nakata[4], P. Rosati[5], F. Shankar[6], M. Tanaka[7], H. Ford[8], M. Huertas-Company[1], G. Illingworth[3], T. Kodama[4], M. Postman[9], A. Rettura[2], J. P. Blakeslee[10], R. Demarco[11], M. J. Jee[3] and R. L. White[9]

Abstract. We combine multi-wavelength data of the Lynx superstructure and GOODS/CDF-S to build a sample of 75 visually selected early-type galaxies (ETGs), spanning different environments (cluster/group/field) at $z \sim 1.3$. By estimating their mass, age (SED fitting, with a careful attention to the stellar population model used) and size, we are able to probe the dependence on the environment of the mass-size relation. We find that, for ETGs with $10^{10} < M/M_{\odot} < 10^{11.5}$, (1) the mass-size relation in the field did not evolve overall from $z \sim 1.3$ to present; (2) the mass-size relation in cluster/group environments at $z \sim 1.3$ lies at smaller sizes than the local mass-size relation ($R_{e,z\sim1.3}/R_{e,z=0} \sim 0.6$-$0.8$).

Keywords: galaxies: clusters: individual (RX J0849+4452, RX J0848+4453), galaxies: evolution, galaxies: formation, galaxies: high-redshift, galaxies: fundamental parameters

1 Introduction

In recent years, studies have unveiled the existence at $z \sim$ 1-2 of a population of massive spheroidal galaxies with small size, hence called compact (e.g., Daddi et al. 2005; Buitrago et al. 2008; Cimatti et al. 2008; van Dokkum et al. 2008; Damjanov et al. 2009; Saracco et al. 2010; Strazzullo et al. 2010, and also references therein). When comparing those high redshift galaxies with local ones of similar mass, it appears that their sizes are smaller by a factor of ∼2-3 and up to 5 (van Dokkum et al. 2008).

The formation of compact galaxies might be a consequence of mergers of gas-rich subunits at high redshift (e.g., Khochfar & Silk 2006) and/or cold flows (e.g., Bournaud et al. 2011), resulting in an intense starbust and compact quiescent remnant due to highly dissipative processes. The picture concerning the subsequent evolution of compact galaxies down to $z = 0$ is more difficult to draw. The comparison of high redshift to local samples may be affected by two selection biases: age selection bias against young galaxies in high redshift samples (e.g. Valentinuzzi et al. 2010) and progenitor bias due to morphological evolution (e.g., van Dokkum & Franx 2001). Within this context, it is still unclear which part of the galaxy population went through evolution and which mechanism contributed to it. If the compact galaxy population requires evolution, one efficient process may be minor dry mergers (Naab et al. 2009; Shankar et al. 2011).

[1] GEPI, Observatoire de Paris, Section de Meudon, 5 Place J. Janssen, 92190 Meudon Cedex, France
[2] Department of Physics, University of California, 1 Shields Avenue, Davis, CA 95616, USA
[3] UCO/Lick Observatories, University of California, Santa Cruz 95065, USA
[4] Subaru Telescope, National Astronomical Observatory of Japan, 650 North A'ohoku Place, Hilo, HI 96720, USA
[5] European South Observatory, Karl-Schwarzschild -Str. 2, 85748, Garching, Germany
[6] Max-Planck-Institüt für Astrophysik, Karl-Schwarzschild-Str. 1, 85748, Garching, Germany
[7] Institute for the Physics and Mathematics of the Universe, The University of Tokyo, 5-1-5 Kashiwanoha, Kashiwa-shi, Chiba 277-8583, Japan
[8] Department of Physics and Astronomy, Johns Hopkins University, Baltimore, MD 21218, USA
[9] Space Telescope Science Institute, 3700 San Martin Drive, Baltimore, MD 21218, USA
[10] Herzberg Institute of Astrophysics, National Research Council of Canada, Victoria, BC V9E 2E7, Canada
[11] Department of Astronomy, Universidad de Concepción, Casilla 160-C, Concepción, Chile

To go deeper in understanding these mechanisms, it is useful to study the mass-size relation (MSR) as a function of environment. Until now, few studies have covered the full range of environment when studying the mass-size relation at $z > 1$. In the local universe, Maltby et al. (2010) found that the MSR does not depend on the environment for ETGs.

In Raichoor et al. (2011a), we presented a unique homogeneous sample of ETGs probing cluster, group and field environments at $z \sim 1.3$. Our study relies on high-quality multi-wavelength data covering the Lynx supercluster, a structure at $z = 1.26$ made of two clusters and at least three groups, spectroscopically confirmed (Stanford et al. 1997; Rosati et al. 1999; Nakata et al. 2005; Mei 2011).

We here use this sample to study the influence of environment on the structural parameters of ETGs at high redshift as a function of mass and environment. The estimates of ETG sizes from *HST*/ACS images combined with stellar population parameters (Raichoor et al. 2011a) allow us to build the MSR (Raichoor et al. 2011b).

2 Data and sample selection

This work relies on optical/near-infrared ($Ri_{775}z_{850}JK_s$[3.6μm][4.5μm]) images of the Lynx supercluster (Raichoor et al. 2011a) and of the Great Observatories Origins Deep Survey (GOODS; Giavalisco et al. 2004) observations of the Chandra Deep Field South (CDF-S; Giavalisco et al. 2004; Nonino et al. 2009; Retzlaff et al. 2010, Dickinson et al., in preparation). The sample consists of 75 ETGs (30 in the Lynx clusters, 18 in the Lynx groups and 27 in the CDF-S) selected in redshift ($0.92 \leq z_{phot} \leq 1.36$ for the Lynx ETGs and $1.1 \leq z_{spec} \leq 1.4$ with $\langle z_{spec} \rangle = 1.239 \pm 0.082$ for the CDF-S), in magnitude (z_{850} (AB) ≤ 24) and in morphology (E/S0 types based on visual inspection of z_{850}-band of *HST*/ACS images). ETGs belonging to the Lynx clusters and groups are identified in Mei (2011) by a Friend-Of-Friend algorithm (Geller & Huchra 1983).

At $z_{850} = 24$ mag, Lynx samples are complete and our CDF-S sample is more than 70% complete. The Lynx cluster, group, and CDF-S field samples have similar spectral coverage and are almost complete at $z_{850} = 24$ mag, thus providing a homogeneous and consistent sample. Our sample has spectroscopic redshifts for 20/30 ETGs in the clusters, 8/18 ETGs in the groups (Mei 2011) and 27/27 ETGs in the field.

3 Analysis

We estimate stellar masses and stellar population ages (Raichoor et al. 2011a) by fitting the SED with different stellar population models: Bruzual & Charlot (2003), Maraston (2005), and an updated version [CB07] of Bruzual & Charlot (2003) that implements a new modeling of the TP-AGB phase. We hereafter refer to those models as BC03, MA05 and CB07, respectively. For SED fitting we used a Salpeter (1955) IMF, solar metallicity, exponentially declining star-formation histories $\psi(t) \propto e^{-t/\tau}$ with a characteristic time $0.1 \leq$ SFH τ (Ga) ≤ 5, and no dust.

We estimate the sizes of our ETGs (Raichoor et al. 2011b) in the *HST*/ACS z_{850} band images, the closest to the rest-frame B–band in our sample. We fit with a Sersic (1968) $r^{1/n}$ profile the observed two-dimensional surface brightness distributions, using the GALFIT (Peng et al. 2002) software.

4 Results

4.1 Dependence on the stellar population models

We observe that the difference in predicted masses (and ages) between models depends on the ETG's age, as can be seen in Fig.1, where we plot the ratio of the masses predicted with two models versus the age. The modeling of this TP-AGB phase has a significant impact on the derived masses and ages for galaxies observed at high redshift: BC03 models seem to underestimate the impact of the TP-AGB phase, which explains why the inferred masses (and ages) are higher than those inferred with MA05/CB07 (especially around ~ 1 Ga, where the TP-AGB phase is the more active). While recent models from MA05 and CB07 offer better modeling of the TP-AGB phase with respect to less recent BC03 models, we still observe some discrepancies between their predictions.

4.2 Mass-size relation at $z \sim 1.3$

We plot in Fig.2, for the three environments and the three models, the normalized distributions of the size ratio $R_e/R_{e,Valen.}$, which represents the ratio between the size of our ETGs and the one predicted by the local MSR

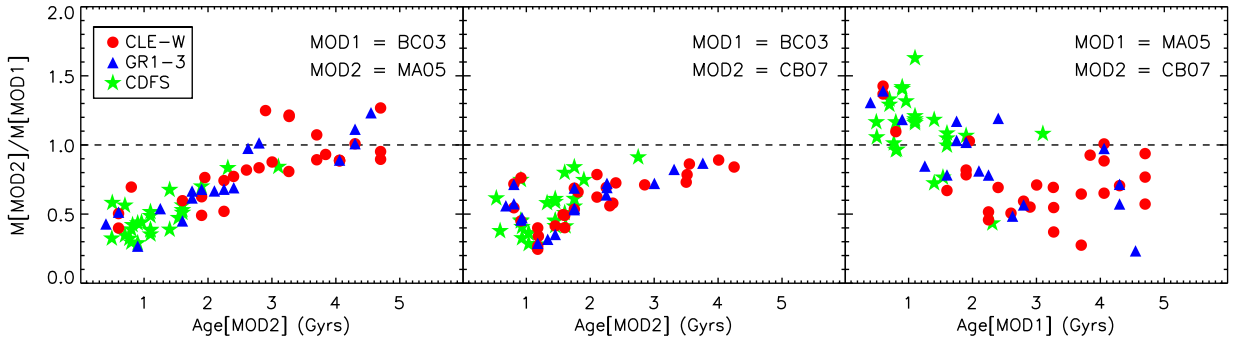

Fig. 1. Dependence of the estimated mass on the stellar population models (BC03/MA05/CB07). Mass ratios as a function of age. Lynx cluster ETGs are the red dots, Lynx group ETGs are the blue triangles and CDF-S ETGs are the green stars. For our sample, typical mass uncertainty is 40%-60% and typical age uncertainty is 1-1.5 Ga.

of Valentinuzzi et al. (2010) at similar masses. Despite the dependence on the model, there is a general trend : most of the cluster and group ETGs lie below local MSRs. We observe that cluster and group size ETG ratios are mostly below 1 with a narrow distribution that peaks around 0.6-0.8, whereas field ETG size ratios have a more widespread distribution, peaking around 0.7-1.1. *At a given mass, ETGs in denser environments tend to have smaller sizes at* $z \sim 1.3$ *than in the local Universe.*

More precisely, when considering stellar masses estimated with MA05/CB07 models, we observe that our field $z \sim 1.3$ ETGs lie on a MSR in agreement with the local one, whereas our cluster/group $z \sim 1.3$ ETGs lie on a MSR with sizes smaller than the local MSR ($R_{e,z\sim1.3}/R_{e,z=0} \sim 0.6$-$0.8$).

When using MA05/CB07 models and looking at the dependence of the size ratio $R_e/R_{e,Valen}$ on the redshift of formation z_{form}, we find that compact ETGs do not have a preferred z_{form} and we observe a near absence of ETGs with $z_{form} > 3$ and a high size ratio ($R_e/R_{e,Valen.} > 2$).

5 Conclusion

We have studied a sample of 75 ETGs spanning a wide range of environments (cluster, group, and field) at $z \sim 1.3$, combining optical/near-infrared observations of the Lynx supercluster, with data on the GOODS/CDF-S field. We estimated the mass and age of our ETGs with SED fitting using BC03, MA05 and CB07 stellar population models, and their size by fitting a Sérsic profile to the *HST*/ACS z_{850} images. We first study the dependence of the derived stellar mass (and age) on the stellar population model used, and then we probe the dependence on the environment of the MSR.

When we compare the MSR of cluster and group ETGs vs field ETGs, we find that, at similar masses, cluster and group ETGs are more compact than field ETGs. Our results are mainly driven by galaxies with masses $M < 2 \times 10^{11} M_{\odot}$. Since in the local Universe, the ETG MSR does not depend on environment, our results imply that, for our mass range ($10^{10} < M/M_{\odot} < 10^{11.5}$), an evolution in the MSR of cluster and group ETG size is required to explain current observations, while field ETGs show a MSR that is compatible with the local one. The evolution of the MSR in dense environments might reflect either an evolution in size of the pristine population or the transformation of ETG progenitors that are not classified as ETG at $z \sim 1.3$ or the accretion of a new population of larger ETGs.

The HAWK-I Distant Cluster Survey (P.I.: C. Lidman), with a multi-wavelength coverage (*HST*, VLT, *Spitzer*) of 10 rich clusters between $z = 0.8$ and $z = 1.4$, will bring crucial observations on the detailed evolution of the MSR in dense environments during a key epoch of galaxy assembly.

References

Bournaud, F., Chapon, D., Teyssier, R., et al. 2011, ApJ, 730, 4
Bruzual, G. & Charlot, S. 2003, MNRAS, 344, 1000
Buitrago, F., Trujillo, I., Conselice, C. J., et al. 2008, ApJ, 687, L61
Cimatti, A., Cassata, P., Pozzetti, L., et al. 2008, A&A, 482, 21

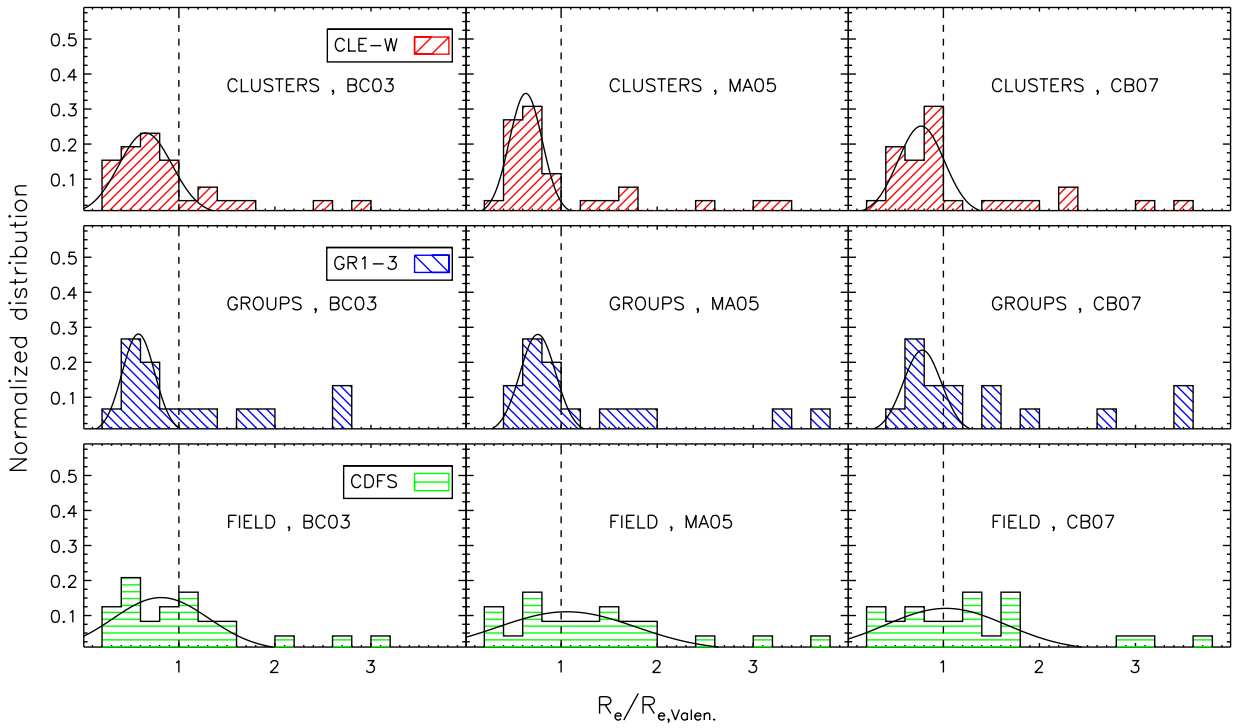

Fig. 2. Size ratio $R_e/R_{e,Valen}$ normalized distributions derived with the three stellar population models (BC03/MA05/CB07), split by environments: Lynx cluster ETGs (*top panels*), Lynx group ETGs (*middle panels*) and CDF-S ETGs (*bottom panels*). $R_e/R_{e,Valen}$ represents the ratio between the size of our ETGs and the one predicted by the local MSR of Valentinuzzi et al. (2010). The black solid line represents the best-fit gaussian to the distributions.

Daddi, E., Renzini, A., Pirzkal, N., et al. 2005, ApJ, 626, 680
Damjanov, I., McCarthy, P. J., Abraham, R. G., et al. 2009, ApJ, 695, 101
Geller, M. J. & Huchra, J. P. 1983, ApJS, 52, 61
Giavalisco, M., Ferguson, H. C., Koekemoer, A. M., et al. 2004, ApJ, 600, L93
Khochfar, S. & Silk, J. 2006, MNRAS, 370, 902
Maltby, D. T., Aragón-Salamanca, A., Gray, M. E., et al. 2010, MNRAS, 402, 282
Maraston, C. 2005, MNRAS, 362, 799
Mei, S., 2011 ApJ, submitted
Naab, T., Johansson, P. H., & Ostriker, J. P. 2009, ApJ, 699, L178
Nakata, F., Kodama, T., Shimasaku, K., et al. 2005, MNRAS, 357, 1357
Nonino, M., Dickinson, M., Rosati, P., et al. 2009, ApJS, 183, 244
Peng, C. Y., Ho, L. C., Impey, C. D., & Rix, H. 2002, AJ, 124, 266
Raichoor, A., Mei, S., Nakata, F., et al. 2011a, ApJ, 732, 12
Raichoor, A., Mei, S., Stanford, S., et al. 2011b, ApJ, in press, arXiv:1109.0284
Retzlaff, J., Rosati, P., Dickinson, M., et al. 2010, A&A, 511, A50+
Rosati, P., Stanford, S. A., Eisenhardt, P. R., et al. 1999, AJ, 118, 76
Salpeter, E. E. 1955, ApJ, 121, 161
Saracco, P., Longhetti, M., & Gargiulo, A. 2010, MNRAS, 408, L21
Sersic, J. L. 1968, Atlas de galaxias australes (Córdoba: Observatorio Astronómico)
Shankar, F., Marulli, F., Bernardi, M., et al. 2011
Stanford, S. A., Elston, R., Eisenhardt, P. R., et al. 1997, AJ, 114, 2232
Strazzullo, V., Rosati, P., Pannella, M., et al. 2010, A&A, 524, A17+
Valentinuzzi, T., Fritz, J., Poggianti, B. M., et al. 2010, ApJ, 712, 226
van Dokkum, P. G. & Franx, M. 2001, ApJ, 553, 90
van Dokkum, P. G., Franx, M., Kriek, M., et al. 2008, ApJ, 677, L5